OPEN ACCESS
Freely Available Online

JOURNAL OF GLYCOMICS AND METABOLISM
ISSN NO: 2572-5424

RESEARCH ARTICLE
DOI : 10.14302/issn.2572-5424.jgm-16-1352

Synthesis of Labeled Rifabutin Dithiocarbamate: A Potential Mycobacterium Tuberculosis Imaging Agent

Syed Qaiser Shah[1]*, Saima Momin[1]

1. Biochemistry Section, Institute of Chemical Sciences, University of Peshawar, Peshawar, KPK, Pakistan.

Abstract

In this investigation, Rifabutin dithiocarbamate (RFND) was labeled with Technetium-99m (99mTc) using tricarbonyl technique. The labeled RFND was further characterized in terms of radiochemical purity, stability in saline & serum, in vitro bacterial binding, biodistribution in animal model rats and for scintigraphic accuracy in animal model rabbit. Finally different radiobiological characteristics of the 99mTc(CO)3-RFND was compared with the recently reported 99mTc-RFN. It was observed that the dithiocarbamate form of RFN showed better radiochemical purity, stability in saline, bacterial binding, biodistribution and targeted imaging than the recently reported 99mTc-RFN. These better radiobiological parameters posed 99mTc(CO)3-RFND as a more reliable agent for tuberculosis imaging.

Corresponding author: Syed Qaiser Shah, Professor & Head Biochemistry Section, University of Peshawar, Peshawar, KPK, Pakistan, phone: 00 92 91 9216701-20 , 0333 9254009, fax: 00 92 91 9216447 ,

Email: ssqaiser2002@yahoo.com

Running title: MYCOBACTERIUM TUBERCULOSIS IMAGING AGENT

Key words: Rifabutin dithiocarbamate, bacterial binding, biodistribution, scintigraphy

Received : Oct 28, 2016; **Accepted :** Feb 20, 2017; **Published :** Mar 01, 2017;

Introduction

In the last century, one of the major achievements of the scientists is the development of vaccines and antibiotics that up to a higher extent eliminated or managed majority of the infectious diseases. Besides such tremendous achievements in the diagnosis and treatment of infectious diseases, infection still remains the focus of investigators and even these days infection is believed to be the major cause of morbidity and mortality[1–2].

Due to the advancement in clinical pathology, the infectious diseases can be detected through simple laboratory tests and successfully treated with appropriate drugs. However, it is observed that a major fraction of those infections resulting in death could be owing to conditions complicated to detect in its early stages. Early and in time detection in such situations could help in appropriate treatment and hence decrease the chances of death[3–4].

Nuclear Medicine Scintigraphic Technology (NMST) provides a different alternative for localization of suspected bacterial infection due its higher sensitivity. In case of deep tissue infection, bone infection, acute life threatening infections which need early appropriate management e.g appendicitis, severe chronic infections occurring due to drug-resistance; and opportunistic infections in immune-compromised persons, one could take advantage of NMST. Such quarries like infection being there or not and its site, severity and potential cause could be answered by using NMST. However, to reply these quarries accurately, the prerequisite is a reliable radio-drug that can accumulate at the site of infection. The radio-drug intended for scintigraphy must answer the above mentioned quarries, but it shall not be toxic, show higher uptake in the target areas, low dose, and low cost easy availability[5–6].

The reported agents[7–11]and its derivatives[12–25] have shown promising specific target (infectious area) to non-target (non infectious area) ratios in its very early stages, besides normal circulatory and excretory behavior. However, the appearance of multidrug resistant bacteria's like *Mycobacterium tuberculosis* (MBT), is a serious threat for the clinicians to detect and manage such infections in its early time[26].

In this scheme, labeling of Rifabutin dithiocarbamate (RFND) (Figure 1.) with ^{99m}Tc was examined using tricarbonyl technique. The feasibility of the tricarbonyl labeling procedure is based on the poorly attached H_2O of the $^{99m}Tc(OH_2)_3(CO)_3]^+$ precursor which can be easily substituted. The labeled RFND was further characterized in terms of radiochemical purity, stability in saline & serum, *in vitro* bacterial binding, biodistribution in animal model rats and for scintigraphic accuracy in animal model rabbit. Finally different radiobiological characteristics of the $^{99m}Tc(CO)_3$-RFND was compared with the recently reported ^{99m}Tc-RFN[27].

Materials

Rifabutin (RFN) was obtained from Chengdu Yuyang High-Tech Developing Co., Ltd. China, and all chemicals & solvents from Sigma. In this work HPLC of Shimadzu, well counter of Ludlum, Dose calibrator of Capintech and Gamma camera of Nuclearmedizine, were used.

Methods

Derivatization of Rifabutin

Rifabutin (RFN) was derivatized to Rifabutin dithiocarbamate (RFND) using the method reported earlier[28]. Briefly, 0.002 mol of RFND and 2.4 mg of NaOH were mixed in a clean sterilized vial. Thereafter, 22 ml of tetrahydrofuran (THF) was added to the reaction vial followed by shaking for 30 min in an ice bath. Then, 2 ml carbon disulfide (CS_2) was added and left the reaction vial for 8 h in an ice bath for continuous shaking. After that the mixture was processed for

(Continued on page 14)

continuous stirring up to 12 h at room temperature followed by recovery through re-crystallization. The RFND was characterized by advance spectroscopic techniques.

Synthesis of $^{99m}Tc(CO)_3$-RFND & Radiochemical purity

Sodium pertechnetate 1 mCi (0.2 ml) was mixed with 2 mg (dissolved in 0.4 ml normal saline) of RFND followed by pH adjustment (pH 10) using 0.1 mol / L HCL in a clean nitrogen gas filled sterilized vial. Thereafter, the mixture was transferred to an Isolink kit followed by incubation for optimum labeling at 25 °C for 15 min.

High-performance liquid chromatography (HPLC) was used to characterize $^{99m}Tc(CO)_3$-RFND in terms of radiochemical purity by the method reported earlier[16] . Briefly, 10 µL of $^{99m}Tc(CO)_3$-RFND was administered to the HPLC system fitted with UV detector operating at 254, and a flow scintillation counter, C-18 column and binary pump. Thereafter, for 15 min, a flow rate of 1 ml / min the column was eluted with water and methanol (W:M). The effluent was collected in separate vials followed by counting for activity.

***Mycobacterium Tuberculosis* (MBT) Uptake**

MBT uptake of $^{99m}Tc(CO)_3$-RFND was assessed adopting the method reported earlier[28] . Briefly, 0.8 mL acaetic acid (0.01 M) containing approximately 1 x 10^8 colony forming units (CFU) of MBT and 0.2 mL sodium phosphate buffer was incubated at 4 °C for 60 min. The mixture was centrifuged at 1500 rpm for 15 min and after removing the supernatant was re-centrifuged after suspending in 1.5 mL sodium phosphate buffer. Subsequently, the supernatant was removed again and the bacterial pellets were counted for activity.

Biodistribution

The percent *in vivo* uptake of the $^{99m}Tc(CO)_3$-RFND was assessed in healthy and artificially infected animal model rats. The animal was divided into two groups i.e. A and B. To group A animals, approximately 1 x 10^8Colony Forming Units (CFU) in 0.2 mL saline MBT was intramuscularly injected into the left leg of the anaesthetized rat Sprague-Dawley rat (weight range, 200–250g) for creating infection. After eight hours, equimolar amount of sterile oil was injected to the right leg of the same rat for creating inflammation followed by intravenous admission of 0.5 mCi $^{99m}Tc(CO)_3$-RFND. To group B animals, the above process was repeated without administration of MBT. Thereafter, the rats were sacrificed at different intervals after intravenous injection of radio-drug as per procedure of the Pakistan Nuclear Regulatory Authority (PNRA), Ethics Committee, Pakistan Atomic Energy Commission (PAEC). Thereafter, % *in vivo* uptake of the $^{99m}Tc(CO)_3$-RFND in one gram of blood, spleen, stomach, intestine, kidney, infected muscle, inflamed and normal muscle was measured using gamma counter.

Imaging with $^{99m}Tc(CO)_3$-RFND

Healthy rabbits (weight: 3.0 to 4.0 kg) were used in the assessment of imaging profile of the instant radio-drug. 0.5 mL MBT containing 1 x 10^8CFU was injected to the left leg of the healthy rabbit and after 08 h, to the right leg of the same rabbit 0.5 mL sterile oil was injected. Finally, the rabbit was placed face up on the bed of the gamma camera followed by intravenous injection of 2 mCi $^{99m}Tc(CO)_3$-RFND. Whole body images were acquired using Low Energy General Purpose (LEGP) collimator at different intervals.

Statistical Analysis

Results are expressed as % Injected dose / gram or ratios ± SEM and statistical analysis were executed using the student *t* -test

Results and Discussion

Chemistry of $^{99m}Tc(CO)_3$-RFND

Rifabutin (RFN) (Fig. 1 (a)) was derivatized to Rifabutin dithiocarbamate (RFND) Fig. 1(b) followed by labeling

with ^{99m}Tc using tricarbonyl technique giving the proposed structure Fig. 1(c) with tetrahedral geometry and stiochiometery of ligand:^{99m}Tc(CO)$_3$ as 1:2. The two sulfur atoms of the bidentate RFND in the *fac*-[^{99m}Tc (CO)$_3$(H$_2$O)]$^+$ precursor readily displaced H$_2$O to give the required ^{99m}Tc(CO)$_3$-RFND complex.

Synthesis of ^{99m}Tc(CO)$_3$-RFND & Radiochemical Purity

The combined HPLC radiochromatogram of ^{99m}Tc(CO)$_3$-RFND and ^{99m}Tc-RFN is shown in Figure 2. The blue line described ^{99m}Tc-RFN and the red ^{99m}Tc (CO)$_3$-RFND. In both lines (blue and red) two markedly different peaks were observed at different retention

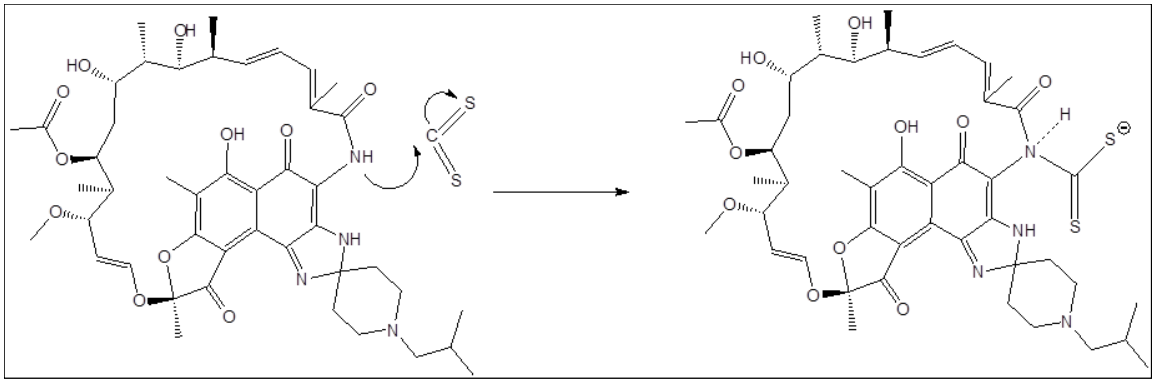

Figure 1 (a). Rifabutin (RFN)

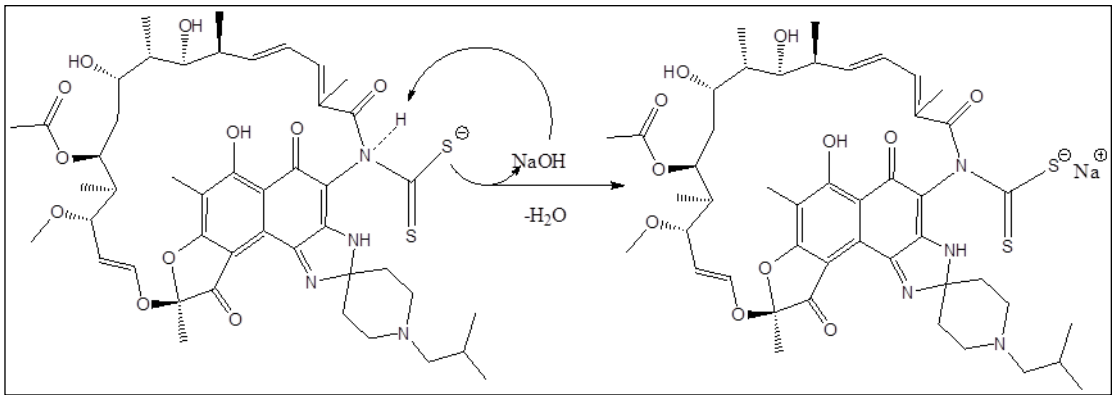

Figure 1(b). Rifabutin dithiocarbamate (RFND)

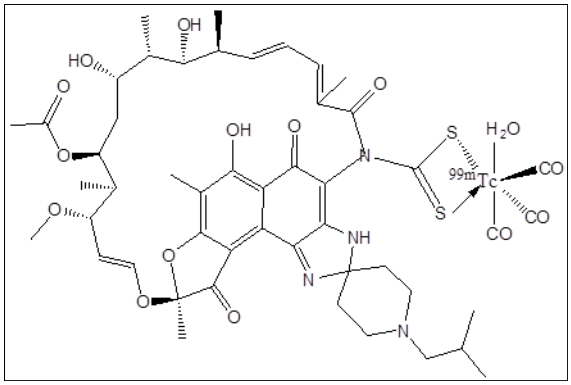

Figure 1 (c). 99mTc(CO)3- RFND complex

times. In blue line signal appear at retention 4.1 min represent the free and hydrolyzed technetium-99m and 11.00 min represent the labeled moiety. The red line also showed two different peaks one at 3.3 and the second at 10.2 min. The signal appear at 3.3 min of retention represent the unlabeled while the one at 10.2 min of retention, the labeled dithiocarbamate.

In normal saline the ^{99m}Tc(CO)$_3$-RFND showed normal profile like ^{99m}Tc-RFN at room temperature up to 240 min after reconstitution. The combine radiochemical stability of ^{99m}Tc(CO)$_3$-RFND and ^{99m}Tc-RFN is shown in Figure 3. The blue trace represent the radiochemical

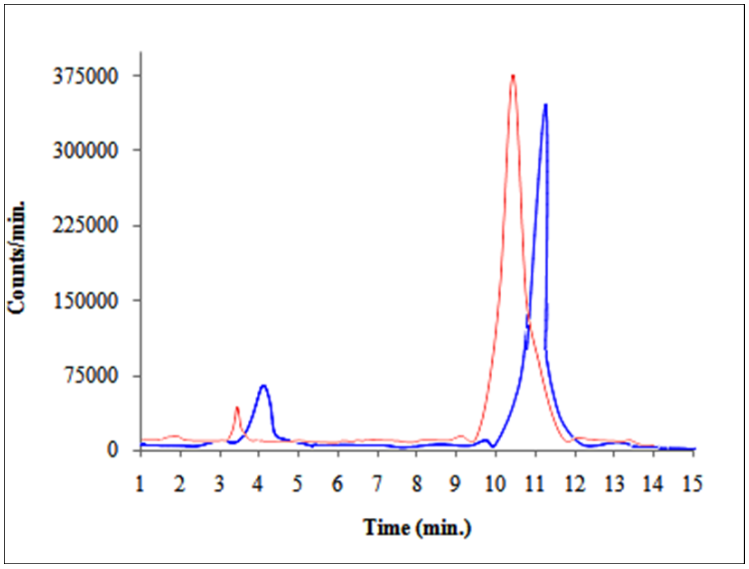

Figure 2. Combined HPLC trace of $^{99m}Tc(CO)_3$- RFND (red trace) and ^{99m}Tc-RFN (blue trace)

stability profile of the $^{99m}Tc(CO)_3$-RFND up to 240 min, wherein it was observed that the $^{99m}Tc(CO)_3$-RFND has shown more than 90 % stability. In normal saline the observed radiochemical purities at 1, 30, 60, 90, 120 and 240 min after reconstitution were 94.70 ± 0.24, 99.25 ± 0.20, 98.00 ± 0.18, 96.40 ± 0.00, 95.00 ± 0.16 and 93.10 ± 0.20 %.

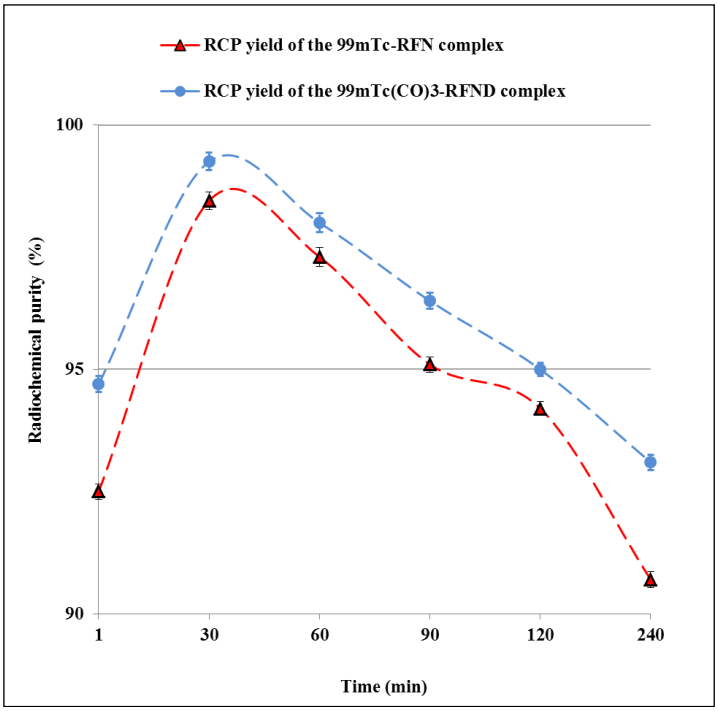

Figure 3. Stability of $^{99m}Tc(CO)_3$-RFND (blue trace) & ^{99m}Tc-RFN (red trace) in normal saline at room temperature

However, the red trace showed radiochemical profile of the ^{99m}Tc-RFN in normal saline up to 240 min after reconstitution portray almost similar trailing patron. The radiochemical purities calculated at 1, 30, 60, 90, 120 and 240 min after reconstitution were 92.50 ± 0.16 %, 98.45 ± 0.18 %, 97.30 ± 0.20 %, 95.10 ± 0.16 %, 94.20 ± 0.14 % and 90.70 ± 0.70 % respectively[27]. The ^{99m}Tc-RFN freshly prepared showed more than 90 % radiochemical purity up to 240 min.

Behavior of $^{99m}Tc(CO)_3$-RFND in Human Serum

The combined behavior of the $^{99m}Tc(CO)_3$-RFND and ^{99m}Tc-RFN is shown in Figure 4. The blue trace was represented the behavior of the $^{99m}Tc(CO)_3$-RFND in human serum at 37 °C up to 16 hrs after reconstitution. The profile of $^{99m}Tc(CO)_3$-RFND at 0, 2, 4, 6, 8, 10, 12, 14 and 16 hrs after reconstitution were 99.00 ± 0.50, 96.15 ±0.44, 93.20 ± 0.42, 91.70 ± 0.44, 90.00 ± 0.46, 88.35 ± 0.40, 87.15 ± 0.46, 86.50 ± 0.44 and 85.80 ± 0.48 % (with overall decay of 13.20 ± 0.15 %) respectively

However, the red trace was represented the behavior of the ^{99m}Tc-RFN in human serum at 37 °C up to 16 hrs after reconstitution. The profile of ^{99m}Tc-RFN at at 0, 2, 4, 6, 8, 10, 12, 14 and 16 hrs after reconstitution were 98.15 ± 0.22 %, 93.30 ± 0.18 %, 90.75 ± 0.24 %, 98.10 ± 0.26 %, 88.35 ± 0.18 %, 86.70 ± 0.20 %, 84.10 ± 0.22 %, and 82.95 ± 0.16 % (with overall decay of 15.20 ± 0.45 %) respectively. Both the radiolabeled had shown permissible less than unwanted species than the limit of decay set US and British pharmacopeia.

Mycobacterium Tuberculosis (MBT) Uptake

The combine MBT uptake of $^{99m}Tc(CO)_3$-RFND and ^{99m}Tc labeled is shown in Figure 5. The MBT uptake of $^{99m}Tc(CO)_3$-RFND observed in case of live MBT at 30, 60, 90 and 120 min were 34.50 ± 1.5, 52.50 ± 1.3, 72.25 ± 1.00, and 60.75 ± 1.8 %

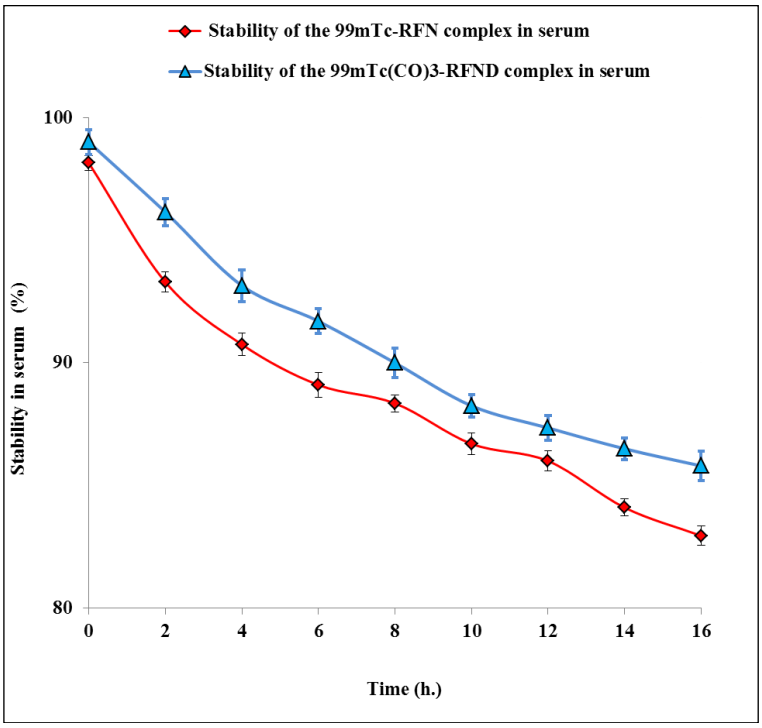

Figure 4. Stability of $^{99m}Tc(CO)_3$-RFND (blue trace) & ^{99m}Tc-RFN (red trace)

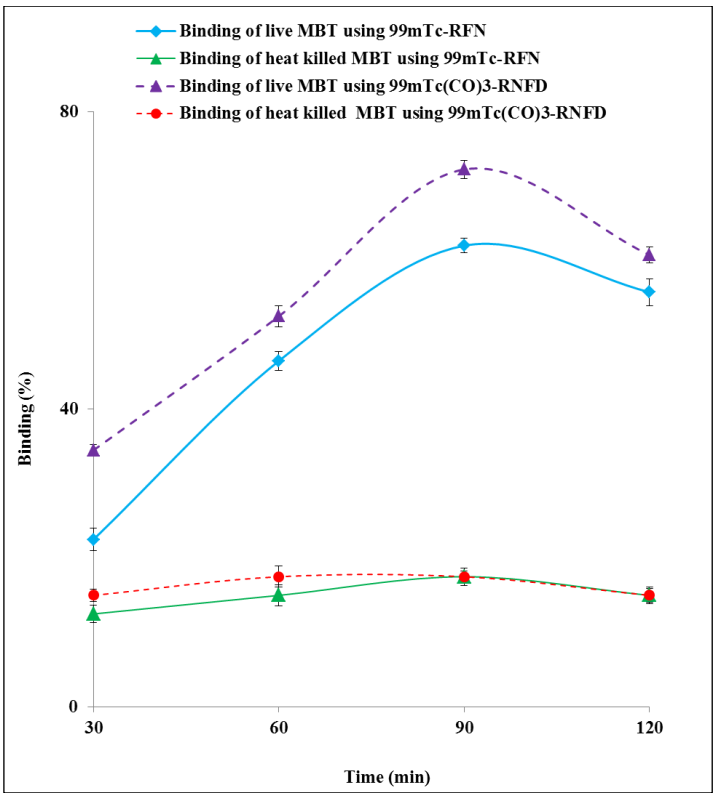

Figure 5. Bacterial binding behavior of 99mTc(CO)3-RFND & 99mTc-RFN

respectively. In case of heat killed MBT the uptake patron of $^{99m}Tc(CO)_3$-RFND showed analogous behavior to the heat killed up take of ^{99m}Tc-RFN. The MBT uptake of $^{99m}Tc(CO)_3$-RFND in case of heat killed MBT recorded at 30, 60, 90 and 120 min were 15.00 ± 1.2, 17.50 ± 1.4, 17.50 ± 0.8 and 15.00 ± 0.9 % respectively. In case of ^{99m}Tc-RFN uptake in live strain of MBT at 30, 60, 90 and 120 min were 22.50 ± 0.8, 46.50 ± 1.4, 62.00 ± 1.2 and 55.75 ± 1.10 % respectively. However, in case of heat killed MBT the uptake patron 30, 60, 90 and 120 min showed close correlation with uptake of $^{99m}Tc(CO)_3$-RFND. The uptake observed in case of heat killed MBT were 12.50 ± 1.5, 15.00 ± 1.2, 17.50 ± 1.00 and 15.00 ± 1.4 respectively. The combine uptake profile of $^{99m}Tc(CO)_3$-RFND and ^{99m}Tc-RFN in MBT (both live and heat killed) demonstrated almost similar uptake behavior[27].

Biodistribution in Animal Model Rats

The percent distribution of $^{99m}Tc(CO)_3$-RFND in one gram of blood, liver, spleen, stomach, intestine, kidney, infected muscle, inflamed and normal muscle of animal model rats is summarized in Table 1. In blood of animal model rats infected with live strain of MBT the activity distribution of $^{99m}Tc(CO)_3$-RFND observed at 30, 60, 90 and 120 min was 21.75 ± 0.24, 10.35 ± 0.22, 9.00 ± 0.28 and 4.35 ± 0.20 %, while in heat killed MBT injected model the distribution observed at 30, 60, 90 and 120 min was 21.25 ± 0.18, 10.75 ± 0.16, 9.20 ± 0.10 and 4.50 ± 0.20 % respectively. In comparison the distribution of ^{99m}Tc-RFN showed almost similar patron, initially a high distribution was noticed which gradually went down from 18.95 ± 0.46, 12.50 ± 0.40, 10.50 ± 0.44 and 6.00 ± 0.34 % respectively. In case of heat killed MBT the distribution of ^{99m}Tc-RFN activity in animal model showed similar behavior as notice in case of $^{99m}Tc(CO)_3$-RFND[27]. No significant change in distribution of activity in different animal models was seen.

The activity distribution of $^{99m}Tc(CO)_3$-RFND in other organs of the animal models have shown almost

Table 1. The percent distribution of 99mTc(CO)3-RFND in animal model rats

Organs /tissues (gm)	Absorption of 99mTc (CO)3 -RFND per gram of different organs at different times							
	In live Mycobacterium tuberculosis				In heat killed Mycobacterium tuberculosis			
Time (min)	30	60	90	120	30	60	90	120
Infected muscle	6.90 ± 0.24	10.50 ± 0.20	15.60 ± 0.18	13.00 ± 0.22	2.00 ± 0.26	2.50 ± 0.22	2.50 ± 0.22	2.00 ± 0.24
Inflamed muscle	3.00 ± 0.10	3.50 ± 0.15	3.00 ± 0.20	3.00 ± 0.15	3.00 ± 0.10	3.50 ± 0.15	3.00 ± 0.20	2.50 ± 0.15
Normal muscle	2.50 ± 0.15	3.00 ± 0.20	2.50 ± 0.20	2.50 ± 0.10	2.50 ± 0.10	3.00 ± 0.16	2.50 ± 0.10	2.50 ± 0.18
Blood	21.75 ± 0.24	10.35 ± 0.22	9.00 ± 0.28	4.35 ± 0.20	21.25 ± 0.18	10.75 ± 0.16	9.20 ± 0.10	4.50 ± 0.20
Liver	20.90 ± 0.16	11.00 ± 0.20	9.50 ± 0.18	5.80 ± 0.14	20.50 ± 0.26	11.45 ± 0.28	9.85 ± 0.22	6.00 ± 0.24
Spleen	10.00 ± 0.28	9.25 ± 0.24	6.15 ± 0.20	4.25 ± 0.28	10.45 ± 0.18	9.55 ± 0.20	6.30 ± 0.16	4.30 ± 0.18
Kidney	9.15 ± 0.24	18.20 ± 0.20	19.10 ± 0.26	22.90 ± 0.28	9.30 ± 0.22	17.65 ± 0.30	20.10 ± 0.24	22.35 ±0.26
Stomach & intestines	9.75 ± 0.34	8.00 ± 0.32	7.10 ± 0.28	4.50 ± 0.30	9.55 ± 0.28	7.85 ± 0.24	6.95 ± 0.22	4.55 ± 0.20

analogous patron as observed in case of ^{99m}Tc-RFN. It was observed that the concentration of the $^{99m}Tc(CO)_3$-RFND in other organs like liver, spleen, stomach and intestine considerably went down up to 120 min after injection. The concentration of $^{99m}Tc(CO)_3$-RFND in liver of animal model infected with live strain of MBT at 30, 60, 90 and 120 min was 20.90 ± 0.16, 11.00 ± 0.2, 09.50 ± 0.18 and 5.80 ± 0.14 % and in animal model infected with heat killed MBT was 20.50 ± 0.26, 11.45 ± 0.28, 9.85 ± 0.22 and 6.00 ± 0.24 % respectively. The distribution of $^{99m}Tc(CO)_3$-RFND in liver (one gram) of animal models have shown similar behavior with no significant difference with the reported radio-labeleds. The quantity of ^{99m}Tc-RFN observed in liver of animal models infected with live strain at different intervals were 18.95 ± 0.46 %, 12.50 ± 0.40 %, 10.50 ± 0.44 % and 6.00 ± 0.34 %, while in case of animal model infected with heat killed strain of MBT 18.50 ± 0.38 %, 12.40 ± 0.38 %, 10.30 ± 0.40 %, and 6.10 ± 0.30 % respectively[27].

A similar distribution patron has been observed in spleen of animal models. The activity distribution of $^{99m}Tc(CO)_3$-RFND observed in spleen of animal model infected with live strain of MBT at 30, 60, 90, and 120 min was 10.00 ± 0.28, 9.25 ± 0.24, 6.15 ± 0.20 and 4.25 ± 0.28 % while in model infected with heat killed MBT was 10.45 ± 0.18, 9.55 ± 0.20, 6.30 ± 0.16 and 4.30 ± 0.18 % respectively. The distribution of $^{99m}Tc(CO)_3$-RFND activity in animal models have shown similar patron what we had observed in case of ^{99m}Tc-RFN. The level of activity seen in animal model infected with live strain of MBT in case of ^{99m}Tc-RFN at at 30, 60, 90, and 120 min were 10.15 ± 0.38 %, 9.85 ± 0.40 %, 6.90 ± 0.36 % & 4.50 ± 0.38 % and in heat killed MBT model was 9.95 ± 0.55 % 9.35 ± 0.30 %, 6.80 ± 0.50 %, and 4.30 ± 0.44 %

In stomach and intestine a similar distribution of $^{99m}Tc(CO)_3$-RFND was seen, as what we had observed in case of ^{99m}Tc-RFN. The activity distribution of $^{99m}Tc(CO)_3$-RFND in animal model infected with live and heat killed MBT at 30, 60, 90, and 120 min were 9.75 ± 0.34, 8.00 ± 0.32, 7.10 ± 0.28 and 4.50 ± 0.30 % and 9.55 ± 0.28, 7.85 ± 0.24, 6.95 ± 0.22 and 4.55 ± 0.20 % respectively. The activity distribution of $^{99m}Tc(CO)_3$-RFND showed close correlation to ^{99m}Tc-RFN. In animal model infected with live and heat killed MBT the activity distribution reported at at 30, 60, 90, and 120 min were 9.50 ± 0.30 % 7.80 ± 0.34 % 6.75 ± 0.36 % and 4.30 ± 0.36 % and 8.95 ± 0.30 %, 7.55 ± 0.34 %, 6.45 ± 0.38 %, and 4.40 ± 0.36, respectively.

The distribution of $^{99m}Tc(CO)_3$-RFND in kidney showed similar patron as what we had observed in reported RFN[27]. It was observed that the activity level was high initially which later on went down. No considerable alterations were observed of activity distribution in animal models infected with live or heat killed MBT. The quantity of $^{99m}Tc(CO)_3$-RFND activity at 30, 60, 90, and 120 min in animal models infected with live and heat killed MBT were 9.15 ± 0.24, 18.20 ± 0.20, 19.10 ± 0.26, 22.90 ± 0.28 and 9.30 ± 0.22, 17.65 ± 0.30, 20.10 ± 0.24 and 22.35 ± 0.26 % respectively. However, using ^{99m}Tc-RFN more or less similar results were reported in animal model rats infected with either live and heat killed pathogen.

In animal model rats infected with live strains of MBT it was observed that the distribution of $^{99m}Tc(CO)_3$-RFND activity in the infected muscle was low in preliminary stages, which went up gradually. The recorded activity distribution at 30, 60, 90, and 120 min were 6.90 ± 0.24, 10.50 ± 0.20, 15.60 ± 0.18 and 13.00 ± 0.22 % respectively. However, in animal model infected with heat killed MBT the level at 30, 60, 90, and 120 min were 2.00 ± 0.26, 2.50 ± 0.22, 2.50 ± 0.22 and 2.00 ± 0.24 % respectively. Further, the reported distribution of 99mTc-RFN in animal model infected with live and heat killed pathogen at 30, 60, 90, and 120 min were 5.85 ± 0.44 %, 09.15 ± 0.30 %, 14.15 ± 0.00,

12.85 ± 0.40 and 2.50 ± 0.45 % 3.00 ± 0.50 %, 3.50 ± 0.45 %, and 3.00 ± 0.00 respectively[27].

Similarly inconsequential deviations were observed in the distribution of $^{99m}Tc(CO)_3$-RFND activity in the other muscles of the animal models (inflamed and normal). Further, higher distribution of $^{99m}Tc(CO)_3$-RFND in the inflamed muscle was observed in contrast to the normal. However, the level of $^{99m}Tc(CO)_3$-RFND in both muscles went down gradually. The level of $^{99m}Tc(CO)_3$-RFND distribution observed at 30, 60, 90, and 120 min in the inflamed muscle of the animal model infected with live and heat killed MBT were 3.00 ± 0.10, 3.50 ± 0.15, 3.00 ± 0.20, 3.00 ± 0.15 and 3.00 ± 0.10, 3.50 ± 0.15, 3.00 ± 0.20 and 2.50 ± 0.15 % respectively. In case of

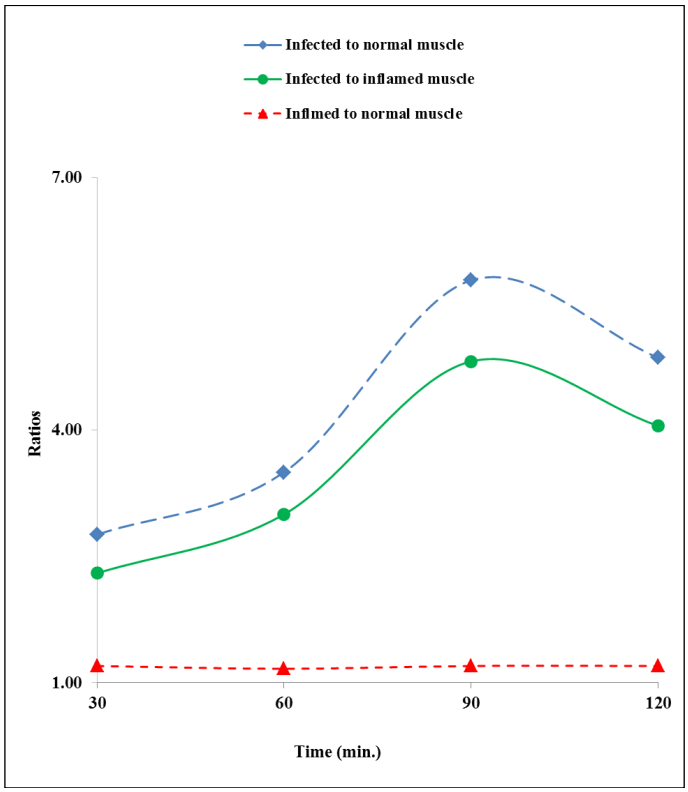

Figure 6. Uptake of $^{99m}Tc(CO)_3$-RFND in muscles.

^{99m}Tc-RFN, the distribution of activity showed almost similar patron. The level of ^{99m}Tc-RFN activity reported in the inflamed muscles of the animal models infected with live and heat killed pathogens were 3.50 ± 0.40 %, 3.50 ± 0.45 %, 3.50 ± 0.45 %, 3.00 ± 0.50 and 4.00 ± 0.36 %, 3.50 ± 0.30 %, 3.50 ± 0.00 and 3.00 ± 0.34 % respectively.

`In normal muscles of the animal model rats infected with live and or heat killed pathogen a normal and similar distribution was seen in both cases. The level of $^{99m}Tc(CO)_3$-RFND activity distribution in animal models infected with live and heat killed pathogen at 30, 60, 90, and 120 min were 2.50 ± 0.153.00 ± 0.202.50 ± 0.202.50 ± 0.10 and 2.50 ± 0.103.00 ± 0.162.50 ± 0.10 and 2.50 ± 0.18 % respectively

The distribution of activity (ratio-wise) in terms infected to normal, infected to inflamed and inflamed to normal muscles in animal model rats infected are summarized in Figure 6. It was experiential that the concentration of $^{99m}Tc(CO)_3$-RFND in the infected (with live pathogen) muscle was almost six fold advanced than

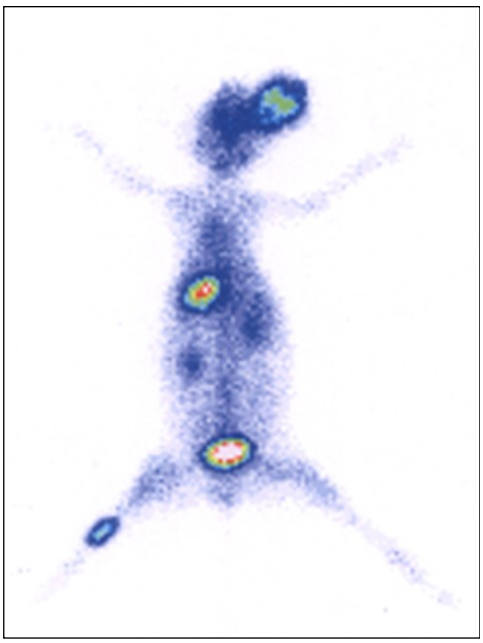

Figure 7. Scintigraphic behavior in animal model

in the normal. Further, the instant profile was not repeated in animal model infected with heat killed pathogen.

Rabbit Scintigraphy

The distribution behavior of $^{99m}Tc(CO)_3$-RFND in animal model infected rabbit with live pathogen is illustrated in Figure 7. After I.V. injection of $^{99m}Tc(CO)_3$-

RFND an improved distribution in various organs was observed in comparison with the reported antibiotics. Initially the concentration of $^{99m}Tc(CO)_3$-RFND activity in the infected muscle was lower which went up significantly with time. However, a considerable variation was seen in the distribution of $^{99m}Tc(CO)_3$-RFND activity infected, inflamed and normal muscle even in early phase of the I.V. administration. After 90 min appreciably higher accumulation of $^{99m}Tc(CO)_3$-RFND was observed in the infected muscle and clearly visualized affected area of the rabbit muscle . Further, it was noted that the concentration of $^{99m}Tc(CO)_3$-RFND in blood, liver and spleen was greater in early phases which fade away with and come into view in the infected muscle and kidneys.

Conclusion

In this project Rifabutin (RFN) was derivatized to its dithiocarbamate to enhance binding sites on the RFN so as to enhance its labeling capacity for more realiable radiodiagnostic agent. It was observed that the dithiocarbamate form of RFN showed better radiochemical purity, stability in saline, bacterial binding, biodistribution and targeted imaging than the ^{99m}Tc-RFN. These better radiobiological parameters posed $^{99m}Tc(CO)_3$-RFND as a more reliable agent for tuberculosis imaging

References

1. Litzler, PY, Manrique, A, Etienne, M, Salles, A, Edet-Sanson, A, Vera, P, Bessou, JP, Hitzel, A. (2010) Leukocyte SPECT/CT for Detecting Infection of Left-Ventricular-Assist Devices: Preliminary Results Journal of Nuclear Medicine. 51,1044-1048.
2. Nanni, C, Errani, C, Boriani, L, Fantini, L, Ambrosini, V, Boschi, S, Rubello, D, Pettinato, C, Mercuri, M, Gasbarrini, A, Fanti, S. (2010) 68Ga-Citrate PET/CT for Evaluating Patients with Infections of the Bone: Preliminary Results Journal of Nuclear Medicine. 51, 1932-1936.
3. Britton, K E,Vinjamuri, S, Hall, AV, Solanki, K, Siraj, Q H, Bomanji, J, Das, S. (1997) Clinical evaluation of technetium-99m infecton for the localization of bacterial infection. European Journal of Nuclear Medicine. 24,553-556.
4. Mirbolooki, MR, Upadhyay, SK, Constantinescu, CC, Pan, ML, Mukherjee, J. (2014) Adrenergic pathway activation enhances brown adipose tissue metabolism: A [18 F]FDG PET/CT study in mice. Nuclear Medicine and Biology. 41, 10-16.
5. Filippi, L, Uccioli, L, Giurato, L, Schillaci, O. (2009) Diabetic foot infection: usefulness of SPECT/CT for 99mTc-HMPAO-labeled leukocyte imaging. Journal of Nuclear Medicine 50, 1042-1046.
6. Wang, Y, Chen, L, Liu, X, Cheng, D, Liu, G, Liu, Y, Dou, S, Hnatowich, DJ, Rusckowski, M. (2013) Detection of Aspergillus fumigatus pulmonary fungal infections in mice with 99mTc-labeledMORF oligomers targeting ribosomal RNA. Nuclear Medicine and Biology. 40, 89-96.
7. Belloli, S.; Brioschi, A.; Politi, L. S.; Ronchetti, F.; Calderoni, S.; Raccagni, I.; Pagani, A.; Monterisi, C.; Zenga, F.; Zara, G.; Fazio, F.; Mauro, A.; Moresco, R. M. (2013) Characterization of biological features of a rat F98 GBM model: a PET-MRI study with [18F]FAZA and [18F]FDG. Nuclear Medicine and Biology. 40, 831-840.
8. Mirbolooki MR, Constantinescu CC, Pan ML, Mukherjee J. (2011) Quantitative assessment of brown adipose tissue metabolic activity and volume using 18F-FDG PET/CT and β3-adrenergic receptor activation. EJNMMI Research 30, 1-11.
9. Wang, Y.; Chen, L.; Liu, X.; Cheng, D.; Liu, G.; Liu, Y.; Dou, S.; Hnatowich, D. J.; Rusckowski, M. (2013) Detection of Aspergillus fumigatus pulmonary fungal infections in mice with 99mTc-labeled MORF oligomers targeting ribosomal RNA. Nuclear Medicine and Biology. 40, 89-96.

10. Liu, X, Cheng, D, Gray, BD, Wang, Y, Akalin, A, Rusckowski, M, Pak, K.Y, Hnatowich, D J. (2012) Radiolabeled Zn-DPA as a potential infection imaging agent. Nuclear Medicine and Biology. 39, 709-714.

11. Bruggen, W. D.; Bleeker-Rovers, C.P.; Otto, C.; Boerman, O. C.; Gotthardt, M.; Oyen, W.J. G. (2009) PET and SPECT in Osteomyelitis and Prosthetic Bone and Joint Infections: A Systematic Review. Seminars in Nuclear Medicine. 40, 3-15.

12. Martins, APD, Ossojr, JA. (2013) Thermal diffusion of 67Ga from irradiated Zn targets. Applied Radiations and Isotopes. 82, 279-282.

13. Liu, Z, Wyffels, L, Barber, C, Hui, M, Woolfenden, J M. (2011) A (99m)Tc-labeled dual-domain cytokine ligand for imaging of inflammation. Nuclear Medicine and Biology 38, 795-805.

14. Oh, SJ, Ryu, JS, Shin, JW, Yoon, EJ, Ha, J, Cheon, JH, Lee, HK. (2002) Synthesis of 99mTc-ciprofloxacin by different methods and its biodistribution. Applied Radiations and Isotopes. 57, 193-200.

15. Chattopadhyay S, Das, MK, Sarkar, BR, Ramamoorthy, N. (1997). Simple procedure for the preparation of iron-free 67Ga from an irradiated copper target—Use of ascorbic acid. 48, 211-212.

16. Ghany, EA, Kolaly, EMT, Amine, AM, Sayed, AS, Gelil, AF. (2005). Synthesis of 99mTc-pefloxacin: A new targeting agent for infectious foci. Journal of Radioanalytical Chemistry. 266, 131-139.

17. Roohi, S, Mushtaq, A, Jehangir, M, Malik, SA. (2006). Synthesis, quality control and biodistribution of 99mTc-Kanamycin. Journal of Radioanalytical and Nuclear Chemistry. 267, 561-566.

18. Motaleb, MA. (2009) Preparation, quality control and stability of 99mTc-sparafloxacin complex, a novel agent for detecting sites of infection. Journal of labeled Compound and Radiopharmaceuticals 52, 415-418.

19. Lambrecht, F, Yurt, K, Durkan, P. (2008) Preparation, quality control and stability of 99mTc-cefuroxime axetil. Journal of Radioanalytical and Nuclear Chemistry 275, 161-164.

20. Zhang, J, Guo, H, Zhang, S, Lin, Y, Wang, X. (2008) Synthesis and biodistribution of a novel 99mTcN complex of ciprofloxacin dithiocarbamate as a potential agent for infection imaging. Bioorganic & Medicinal Chemistry Letters 19, 5168-5170.

21. Chattopadhyay, S, Das, SS, Chandra, S, De, K, Mishra, M, Sarkar, BR, Sinha, S, Ganguly, S. (2010) Synthesis and evaluation of (99m)Tc-moxifloxacin, a potential infection specific imaging agent. Applied Radiations and Isotopes 68, 314-316.

22. Shah, SQ, Khan, AU, Khan, MR. (2010) Radiosynthesis and biodistribution of (99m)Tc-rifampicin: a novel radiotracer for in-vivo infection imaging. Applied Radiations and Isotopes. 68, 2255-2260.

23. Shah SQ, Khan, MR. (2011) Radiosynthesis and biological evaluation of the (99m)Tc-tricarbonyl moxifloxacin dithiocarbamate complex as a potential Staphylococcus aureus infection radiotracer. Applied Radiations and Isotopes 69, 686–690.

24. Shah, SQ, Khan, AU, Khan, MR. (2011) Radiosynthesis and biological evolution of 99mTc (CO)3–sitafloxacin dithiocarbamate complex: a promising Staphylococcus aureus infection radiotracer. Journal of Radioanalytical and Nuclear Chemistry 288,131–136.

25. Oh, SJ, Ryu, JS, Shin, JW, Yoon, EJ, Ha, J, Cheon, JH, Lee, HK. (2002) Synthesis of 99mTc-ciprofloxacin by different methods and its biodistribution. Applied Radiations and Isotopes. 57,193-200.

26. Kaul, A, Hazari, PP, Rawat, H, Singh, B, Kalawat,

TC, Sharma, S, Babbar, AK, Mishra, AK. (2013). Preliminary evaluation of technetium-99m-labeled ceftriaxone: infection imaging agent for the clinical diagnosis of orthopedic infection. International Journal of Infectious Diseases. 17,263–270.

27. Alam, M. (2014) Synthesis Of 99mtc-Rifabutin: A Potential Tuberculosis Radiodiagnostic Agent. M.Phil thesis.

28. Qaiser, SS, Khan AU, Khan MR. (2010) Synthesis, biodistribution and evaluation of 99mTc-sitafloxacin kit: a novel infection imaging agent. Journal of Radioanalytical and Nuclear Chemistry. 284, 189-193.